The 2018 Structures Congress (Structures18)
Songdo Convensia, Incheon, Korea, August 27 - 31, 2018

Effect of strain rate on the seismic performance of reinforced concrete structure

* Rou-Han Li[1)], Hong-Nan Li[2)] and Chao Li[3)]

[1), 2) , 3)] *State Key Lab. of Coastal and Offshore Engineering, Faculty of Infrastructure Engineering, Dalian University of Technology, Dalian 116024, Liaoning, China*
[2)] *Shenyang Jianzhu University, Shenyang 110168, Liaoning, China*
[1)] *lirouhan@mail.dlut.edu.cn*

ABSTRACT

The mechanical properties of reinforced steel and concrete materials under dynamic loading are quite different as compared with those under quasi-static loading. Thus the rate-sensitivities of materials should be given a rational consideration in the seismic performance assessment of reinforced concrete (RC) structures under seismic loading rate. In this paper, the influences of strain rate effect on the dynamic behaviours of RC structure are numerically investigated. Based on an effective approach for considering strain rate effect in the nonlinear analyses of RC structures, the rate-independent and rate-dependent models of an exemplar RC frame structure designed according to the Chinese seismic design code (GB50011-2010) are established on the OpenSees platform and earthquakes with different dynamic characteristics are selected as seismic inputs. By comparing the seismic responses of the rate-independent and rate-dependent models through the incremental dynamic analyses, it is indicated that both the types and intensities of ground motions have an influence on the seismic strain rate. Moreover, the strain rate effect has a considerable impact on both the global and local responses of RC structure under seismic excitations. Moreover, it is suggested that the strain rate effect should be taken into account in the structural performance assessment, especially under pulse-like earthquakes with high-intensity levels.

1. INTRODUCTION

In the seismic analyses of reinforced concrete (RC) structures, the quasi-static material properties are commonly used by civil engineers and researchers. However, large numbers of experimental results on RC materials have indicated that the material properties under dynamic loadings, such as earthquake, impact blast may exhibit a significant enhancement of strength as compared with those under static loading (Fu 1991). Moreover, the dynamic behaviors of RC structural members have been experimentally investigated (Adhikary 2012, Ghannoum 2012, Wang 2013). The test

---

[1)] Ph.D candidate
[2)] Professor
[3)] Post-Doctoral Researcher

results showed an increase of yielding capacity, ultimate capacity and initial stiffness of RC structural members under seismic loading rate if compared with those under pseudo-static loading. The strain-rate sensitivity of materials may exert adverse impact on the structural seismic performance, for some experimental observations present an undesirable reduction in the deformation capacity of structural members under dynamic loadings (Al-Haddad 1995).

A number of numerical simulation have been conducted to investigate the influences of strain rate effect on the seismic performance of structures. The dynamic increase factors (DIFs), which are well-established on large numbers of experimental data and applicable to specific types and classes of concrete and steel, are mostly adopted for the consideration of strain rate effect. (Wang 2016) found that by including the strain rate effect, more accurate predictions to the experimental results can be provided. Research by (Li 2012) indicated that with the consideration of strain rate effect, the maximum base shear and moment of base node may increase while the maximum top displacement may decrease. (Asprone 2012) investigated the influences of strain rate effect on the seismic fragility of RC frame structures and a noticeable reduction of exceedance probability for collapse damage state at a strain rate of 10^{-1}/s was obtained as compared with the failure probability at the quasi-static strain. (Pankaj 2005) found the influence of strain rate effect is unobvious as compared with the influence of the seismic uncertainties on the seismic behaviour of a RC frame. It should be noticed that most of the studies use the DIFs with time-varying strain rates which requires large amounts of computation effort. Moreover, they all focus on the normal type of seismic ground motions, i.e. the far-field ground motions.

Up to now, whether or not consider the strain rate effect in the structural seismic analysis is still a controversial issue for the reason that the available dynamic experimental results are insufficient. Thus, this paper numerically investigates the influences of ground motion dynamic characteristics on the strain rate in structural members. Furthermore, strain rate effect on both the global and local responses of RC frame structure under different types and intensities of seismic ground motions are discussed by using the incremental dynamic analysis (IDA) method. And finally, some useful conclusions are drawn.

2. Rate-independent and rate-dependent models

2.1 Rate-dependent material models

Based on different theoretical backgrounds, such as micro-cracking, viscoplasticity and viscoelasticity, numerous material constitutive models have been developed to consider the strain rate effect. However, the DIFs which are defined as the ratio of material properties values under the dynamic loading to the corresponding values under the static loading, are more feasible in the nonlinear dynamic analysis of RC structures. In this paper, by employing the DIFs recommended by the Euro-International Committee for Concrete (1993), modification to a total of six critical material parameters of static constitutive relationships are made to obtain the rate-dependent model, i.e., the concrete compressive strength and strain, concrete tensile strength, compressive and tensile elastic modulus of concrete and yielding strength of reinforcing steel.

Concrete compressive strength The relationship between the DIF of concrete compressive strength and the strain rate provided by the CEB is represented in Eq. (1)

$$\mathrm{DIF}_{f_c} = \frac{f_{cd}}{f_{cs}} = \left(\frac{\dot{\varepsilon}_c}{\dot{\varepsilon}_{c0}}\right)^{1.026\alpha}, \alpha = \frac{1}{(5+9\frac{f_{cs}}{f_0})} \tag{1}$$

where f_{cd} and f_{cs} are the dynamic and quasi-static compressive strength of concrete in MPa, respectively; $\dot{\varepsilon}_c$ is the dynamic compressive strain rate in 1/s and $\dot{\varepsilon}_{c0}$ is the quasi-static compressive strain rate, which is assumed to be 3.0×10^{-5}/s in this study; f_0 is a constant equal to 10 MPa.

Concrete compressive ultimate strain For the ultimate compressive strain of concrete, which is defined as the strain when the stress reaches the peak value, the dependence of DIF on the strain rate recommended by CEB is given in Eq. (2)

$$\mathrm{DIF}_{\varepsilon_{cu}} = \frac{\varepsilon_{cud}}{\varepsilon_{cus}} = \left(\frac{\dot{\varepsilon}_c}{\dot{\varepsilon}_{c0}}\right)^{0.02}, \tag{2}$$

where ε_{cud} and ε_{cus} are the dynamic and quasi-static ultimate compressive strain of concrete, respectively.

Concrete tensile strength The CEB recommendation for the DIF of concrete tensile strength is expressed in Eq. (3)

$$\mathrm{DIF}_{f_t} = \frac{f_{td}}{f_{ts}} = \left(\frac{\dot{\varepsilon}_t}{\dot{\varepsilon}_{t0}}\right)^{1.0\delta 6}, \delta = \frac{1}{(10+6\frac{f_{cs}}{f_0})} \tag{3}$$

where f_{td} and f_{ts} are the dynamic and quasi-static tensile strength of concrete in MPa, respectively; $\dot{\varepsilon}_t$ is the dynamic tensile strain rate and $\dot{\varepsilon}_{t0}$ is the quasi-static tensile strain rate, which is assumed to be 3.0×10^{-6}/s.

Concrete elastic modulus The tensile and compressive elastic modulus of concrete under the dynamic loading condition are also modified and the corresponding DIF values provided by CEB relationships are expressed in Eqs. (4) and (5).

$$\mathrm{DIF}_{E_c} = \frac{E_{cd}}{E_{cs}} = \left(\frac{\dot{\varepsilon}_c}{\dot{\varepsilon}_{c0}}\right)^{0.026}, \tag{4}$$

$$\mathrm{DIF}_{E_t} = \frac{E_{td}}{E_{ts}} = \left(\frac{\dot{\varepsilon}_t}{\dot{\varepsilon}_{t0}}\right)^{0.016}, \quad (5)$$

where E_{cd} and E_{cs} are the dynamic and quasi-static compressive elastic modulus in MPa, respectively; E_{td} and E_{ts} are the dynamic and quasi-static tensile elastic modulus in MPa, respectively.

Yielding strength of reinforcing steel The DIF value provided by the CEB relationship is expressed in Eq. (6)

$$\mathrm{DIF}_{E_c} = \frac{E_{cd}}{E_{cs}} = \left(\frac{\dot{\varepsilon}_c}{\dot{\varepsilon}_{c0}}\right)^{0.026}, \quad (6)$$

where f_{yd} and f_{ys} are the dynamic and quasi-static yielding strength of reinforcement, respectively; $\dot{\varepsilon}_s$ is the dynamic strain rate of steel; and $\dot{\varepsilon}_{s0}$ is a constant value equal to 5.0×10-5/s.

2.2 Approach for considering strain rate effect

To consider the strain rate effect in the nonlinear time history analyses of RC structures, two approaches are available in current literature. One is to modify the material properties after each analysis step using the DIFs computed by the real-time strain rates (Pankaj 2005), and the other is to use a constant strain rate for a rough consideration of the rate-sensitivity of RC materials (Asprone 2012, Wang 2016). On one hand, the real-time updating of strain rates in the first approach requires a high-volume computation, thus making it unsuitable for the seismic fragility assessment of RC structures. On the other hand, the simplification of using constant strain rates may lead to erroneous structural seismic performance predictions for the reason that the variations of strain rates for different structural members under different input ground motions are not taken into account. To reach a compromise between computation accuracy and efficiency, (Li 2018) proposed a novel two-phase approach in assessing the seismic performance of RC structures with the inclusion of strain rate effect and its effectiveness has been verified with the dynamic loading test results of RC columns.

In the first stage of the proposed approach, the calculated strains of longitudinal reinforcement fibers are employed to represent the strain state at each integrated section. The strain rate time histories of structural members can be obtained by taking the derivative of the corresponding calculated strains. The maximum strain rate of each RC frame member is extracted and employed to calculate the DIF values for different material parameters of concrete and reinforcing steel. In the second stage, seismic response and fragility analyses of the updated finite element model of the RC frame structure are carried put with the consideration of strain rate effect. The influences of member location, input earthquake type and ground motion intensity on the strain rates are considered which can ensure the computation accuracy as compared to the method using a constant strain rate. It should be noted that using the maximum strain

rate of each structural member can result in the largest impact of strain rate effect on the structural seismic performance, which corresponds to the unsafe margin of the structural performance.

3. Structural model and ground motions

3.1 RC frame model

To investigate the effect of stain rate on the seismic performance of RC frame structures, an actual 8-story RC frame building designed according to the Chinese seismic design code (GB50011-2010) is selected. The plan and elevation views of the exemplar RC frame and the cross sectional details of structural members are shown in Fig. 1. The standard cube compressive strength of concrete in columns and beams is 30 MPa, whereas the standard yielding strengths of longitudinal reinforcement and stirrup are 400 MPa and 335 MPa, respectively. The OpenSees platform is used for numerical modeling and analysis in this study. The RC column specimens are modeled with the flexibility-based beam-column elements. The uniaxial material Concrete04 in OpenSees, which is based on the model proposed by Popovics and the modified Kent–Park model, is used to model both the unconfined and confined concrete fibers. The reinforcement fibers are modeled with the uniaxial material ReinforcingSteel. In the numerical modeling, the bottom columns are fixed to the foundation and the beam-column joints are assumed to be rigid. Moreover, the second-order deformations due to the P-Δ effect are taken into account.

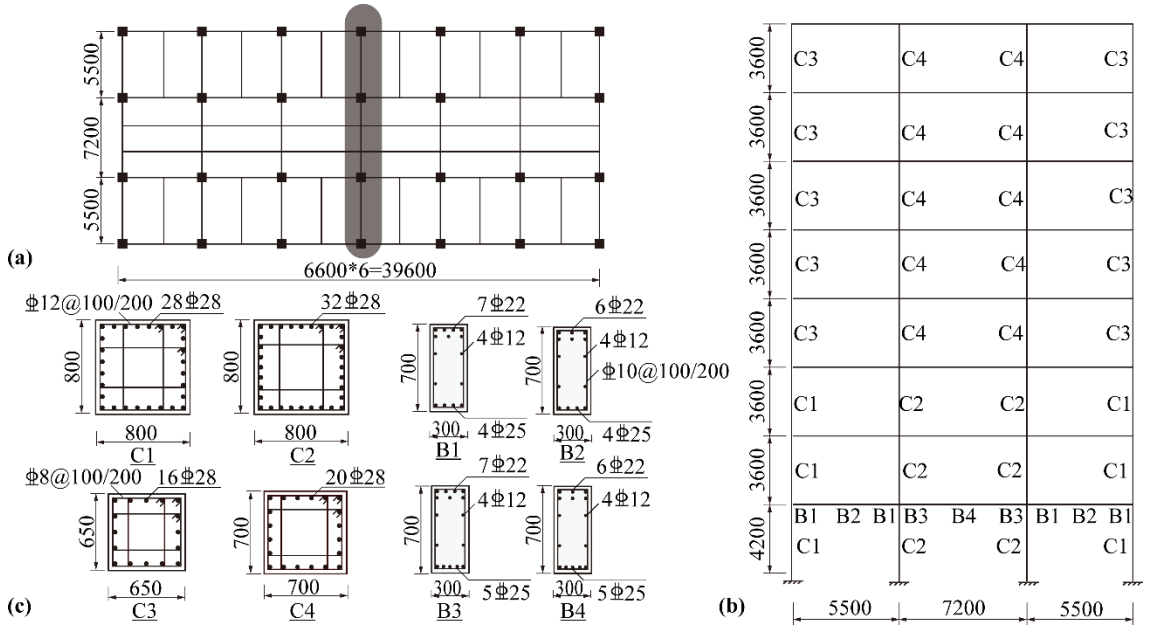

Fig. 1 Structural configurations: (a) plan view; (b) elevation view; and (c) reinforcement layout

3.2 Selected ground motions

In this paper, three suits of ground motions (i.e., far-field, near-field non-pulse-like and near-field pulse-like ground motions) are selected from the PEER-NGA database

(http://ngawest2.berkeley.edu/) to be compatible with the response spectrum defined in the Chinese code for seismic design of buildings. For each suit, a total of 20 ground motions are selected. The ground motions having an epicentral distance less than 20km are considered to be the near-field earthquakes in this study (Stewart 2002). Furthermore, the ground motion is taken as a pulse-like record if the ratio of peak ground acceleration (PGA) to peak ground velocity (PGV) is larger than 0.2/s; otherwise it is a non-pulse-like record (Liao 2004).

4. Influences of ground motions on strain rate

In the nonlinear time history analyses, the PGAs of input ground motions are scaled from 0.1g to 1.0g with an increment of 0.1g. Under the excitations of different types of ground motions with various PGA*s*, the means and standard deviations (σ) of the maximum strain rates for the structural column and beam elements are summarized in Tab. 1 and Tab. 2, respectively.

Tab. 1 Statistics of the maximum strain rate in column elements (Unit: 1/s)

PGA	Far-field EQ		Near-field EQ		Near-field-P EQ	
	Mean	σ (%)	Mean	σ (%)	Mean	σ (%)
0.1g	2.60E-03	0.08	2.46E-03	0.09	3.93E-03	0.15
0.2g	6.10E-03	0.14	6.23E-03	0.18	8.60E-03	0.57
0.3g	8.58E-03	0.18	9.47E-03	0.24	1.38E-02	1.37
0.4g	1.11E-02	0.24	1.39E-02	0.78	2.98E-02	2.63
0.5g	1.48E-02	0.60	1.89E-02	1.35	4.97E-02	3.65
0.6g	1.92E-02	1.33	2.85E-02	2.59	7.51E-02	4.90
0.7g	2.22E-02	1.54	3.81E-02	3.27	1.07E-01	6.15
0.8g	2.59E-02	1.52	5.23E-02	4.35	1.34E-01	6.28
0.9g	2.90E-02	1.46	6.40E-02	5.11	1.65E-01	7.17
1.0g	3.41E-02	1.54	7.60E-02	5.58	1.97E-01	7.46

Tab. 2 Statistics of the maximum strain rate in beam elements (Unit: 1/s)

PGA	Far-field EQ		Near-field EQ		Near-field-P EQ	
	Mean	σ (%)	Mean	σ (%)	Mean	σ (%)
0.1g	4.98E-03	0.09	5.18E-03	0.18	7.16E-03	0.30
0.2g	1.02E-02	0.29	9.85E-03	0.30	1.52E-02	0.53
0.3g	1.57E-02	0.32	1.43E-02	0.40	2.35E-02	0.74
0.4g	2.14E-02	0.44	1.97E-02	0.53	3.47E-02	3.09
0.5g	2.75E-02	0.60	2.56E-02	0.68	5.08E-02	4.97
0.6g	3.36E-02	0.72	3.22E-02	0.95	6.38E-02	5.23
0.7g	3.91E-02	0.70	3.79E-02	1.18	1.03E-01	9.27
0.8g	4.42E-02	0.78	4.34E-02	1.32	1.25E-01	11.68
0.9g	5.08E-02	1.00	4.85E-02	1.54	1.52E-01	13.95
1.0g	5.65E-02	1.18	6.22E-02	3.67	2.01E-01	13.77

It can be observed that the means and standard deviations of the maximum strain rates are basically magnified with the increase of PGA for both of the column and beam elements. The magnitudes of maximum strain rate values obtained from the numerical simulation range from 10^{-3}/s to 10^{-1}/s, which are in accordance with the experimental results of a shaking table test conducted by Zhang (2011). When the value of PGA is

relatively low, the maximum strain rates of column elements are much smaller than those of beam elements; however, the disparities become smaller with the increase of PGA, and the maximum strain rates of column elements approach or even exceed those of the beam elements when the PGA reaches 1.0g. In other words, the strain rates of column elements are more sensitive to the intensities of input ground motions as compared with those of beam elements.

It can be also found that the strain rates of column and beam elements induced by the far-field ground motions are much smaller than those induced by the near-field pulse-like ground motions. Moreover, the increase of strain rates under the near-field pulse-like ground motions is much more obvious than that under the far-field ground motions for both of the column and beam elements. This is because the strong and long-period pulse in the near-field ground motion can generate high seismic demands that force the frame to dissipate this input ground motion energy with large structural displacements, and result in a much higher maximum strain rate in the column and beam elements as compared with those induced by the far-field and near-field ground motions with no pulse.

5. Strain rate effect on the structural seismic performance

5.1 Strain rate effect on time-history responses

The base shear and top displacement time-histories of the RC frame model subjected to different types of earthquake ground motions are presented in Fig. 2 and Fig. 3, respectively. For each suit of earthquake records, a representative input ground motion with PGA of 0.5g is selected to calculate the structural seismic response. It can be found that the inclusion or exclusion of strain rate effect makes little difference to the frequency contents of the structural responses of base shear and top displacement. The maximum base shears of the rate-dependent model (Model-2) slightly increase as compared with the rate-independent model (Model-1); however, the computed maximum top displacements of Model-2 are lower than those of Model-1.

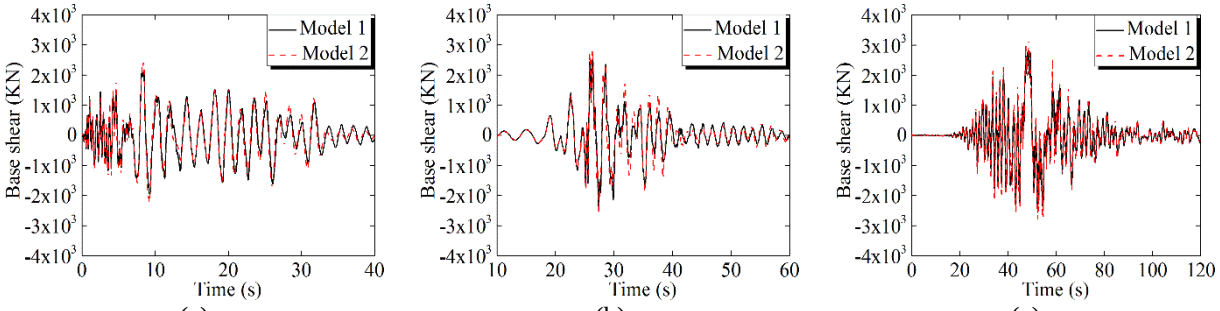

Fig. 2 Comparisons of base shear time-history (PGA=0.5g): (a) far-field EQ-NO.5; (b) near-field EQ-NO.10; and (c) near-field-P EQ-NO.20

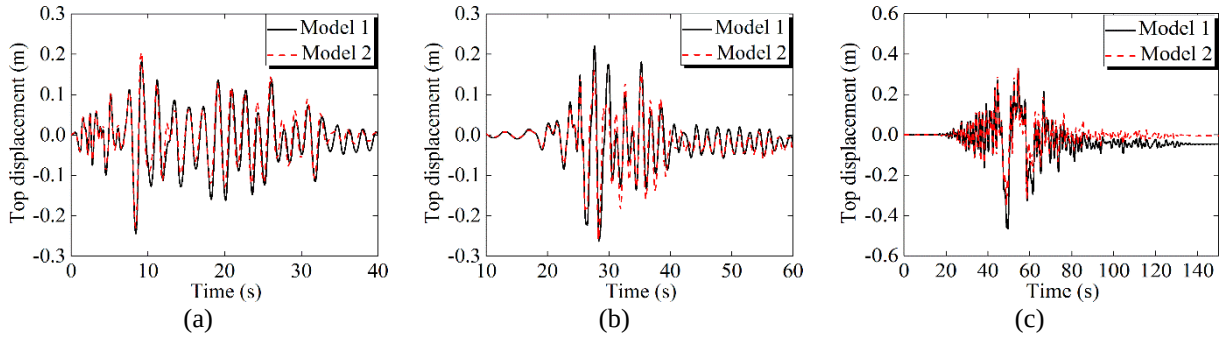

Fig. 3 Comparisons of top displacement time-history (PGA=0.5g): (a) far-field EQ-NO.5; (b) near-field EQ-NO.10; and (c) near-field-P EQ-NO.20

5.2 Strain rate effect on global responses

To quantify the influence of strain rate effect on the structural seismic response, the average maximum values of the base shear and top displacement under different types of ground motions with various intensities are statistically calculated based on the simulation results, as summarized in Tab. 3 and Tab. 4, respectively.

Tab. 3 Comparisons of average maximum base shear with PGA (Unit: KN)

PGA	Far-field EQ			Near-field EQ			Near-field-P EQ		
	Model-1	Model-2	δ (%)	Model-1	Model-2	δ (%)	Model-1	Model-2	δ (%)
0.1g	800.8	829.8	3.62	798.5	795.1	-0.43	1187.0	1217.5	2.57
0.2g	1459.7	1535.0	5.16	1451.6	1489.0	2.58	1951.3	2085.1	6.86
0.3g	1904.7	2049.4	7.60	1956.7	2004.6	2.45	2348.6	2541.5	8.21
0.4g	2170.2	2379.7	9.65	2267.4	2404.2	6.03	2630.0	2887.6	9.79
0.5g	2350.2	2598.5	10.57	2485.8	2641.0	6.24	2783.4	3108.6	11.68
0.6g	2461.3	2745.8	11.56	2658.6	2841.8	6.89	2856.1	3250.4	13.81
0.7g	2543.0	2833.4	11.42	2782.2	3014.7	8.36	2945.2	3339.7	13.39
0.8g	2646.1	2928.6	10.68	2876.0	3153.4	9.64	2972.0	3490.5	17.45
0.9g	2758.8	3016.1	9.32	2951.3	3268.7	10.75	3038.3	3536.8	16.41
1.0g	2885.3	3128.0	8.41	3110.5	3354.5	7.84	3051.2	3541.1	16.06

Tab. 4 Comparisons of average maximum top displacement with PGA (Unit: mm)

PGA	Far-field EQ			Near-field EQ			Near-field-P EQ		
	Model-1	Model-2	δ (%)	Model-1	Model-2	δ (%)	Model-1	Model-2	δ (%)
0.1g	52.9	52.4	-0.95	46.4	45.3	-2.62	84.8	80.8	-4.67
0.2g	107.4	104.1	-3.07	93.1	90.7	-2.61	169.2	164.4	-2.87
0.3g	155.6	154.5	-0.71	137.0	135.7	-0.96	250.3	243.8	-2.59
0.4g	198.9	198.0	-0.45	181.9	177.4	-2.55	397.3	354.3	-10.80
0.5g	245.8	241.5	-1.75	227.8	221.3	-2.92	493.9	421.8	-14.59
0.6g	291.6	287.3	-1.47	275.6	266.7	-3.34	660.2	577.3	-12.55
0.7g	342.2	331.7	-3.07	345.1	314.4	-9.76	867.0	769.3	-11.27
0.8g	398.5	376.8	-5.45	434.6	378.6	-14.78	1049.4	923.0	-12.04
0.9g	447.3	431.5	-3.53	536.2	464.5	-15.43	1367.5	1115.0	-18.46
1.0g	491.6	485.2	-1.30	643.2	560.7	-14.71	1642.9	1329.7	-19.06

It can be observed that in general, the peak base shear increases and the top displacement decreases with the consideration of strain rate effect. These conclusions

are consistent with the available research findings (Li 2012, Pankaj 2005). Basically, with the increase of input ground motion intensity, the relative difference (δ) between the calculated seismic responses of rate-dependent Model-2 and rate-independent Model-1 increases.

Under far-field ground motions, the influence of strain rate effect on the top displacement (-5.45% <δ< -0.45%) is much smaller as compared with the base shear (3.62% <δ< 11.56%); however, the structural base shear and top displacement are both significantly influence by the strain rate effect for the near-field ground motion input cases. Moreover, it can be found that the values of δ under near-field pulse-like ground motions are much larger than those under far-field ground motions. For instance, when PGA equals 1.0g, the values of δ for the average maximum base shear and top displacement under far-field ground motions are respectively 8.41% and -1.30%, but the corresponding values of δ are 16.06% and -19.06% under near-field pulse-like ground motions, respectively. Therefore, it can be concluded that the strain rate effect on structural seismic responses is more evident when the RC frame structure is subjected to near-field pulse-like ground motions.

5.3 Strain rate effect on local damage

In this study, the influence of strain rate effect on the local damage of RC frame structure is investigated by using the average curvature ductility of different structural members ($\bar{\mu}$) as the damage index, i.e. the average value of the ratios of the maximum curvature to the yielding curvature of specific structural member under each suite of earthquake records, which can be calculated by Eq. (7)

$$\bar{\mu} = \frac{1}{N}\sum_{i=1}^{N}\frac{\varphi_{\max}}{\varphi_{y}}, \tag{1}$$

where φ_{y} represents the yielding curvature obtained from the moment-curvature analysis of the corresponding RC section; $\varphi_{\max,i}$ is the maximum structural member curvature determined through the nonlinear dynamic analysis of the structure under the *i*th ground motion; and *N* is the number of input ground motions.

The local damage conditions of the whole structure for Model-1 and Model-2 under three types of ground motions (i.e., the far-field EQ, near-field EQ and near-field-P EQ) with PGA of 0.5g are shown in Fig. 4. By comparing Figs. 4(a) and 4(b) with Figs. 4(d) and 4(e), it can be seen that under far-field and near-field non-pulse-like ground motions, the local damage distribution of structural members calculated by using the rate-dependent model differs slightly from that of the reference model, and most plastic hinges appear at the beam ends and the bottom ends of the first-story columns. It can be observed from Figs. 4(c) and 4(f) that the near-field pulse-like ground motions can exert the most severe structural damage among the three types of input ground motions, the local damage of both beam and column elements under near-field pulse-like ground motions are much more evident as compare with that under far-field and

near-field non-pulse-like ground motions. Moreover, the strain rate effect has a more significant influence on the structural local damage under near-field pulse-like ground motions. The damage in the beam and column members of Model-1 is more serious than that of Model-2, which can be explained by that more significant strain rate effect leads to a larger increase in the material strength, which finally results in an obvious improvement in the seismic performance of the RC frame structure.

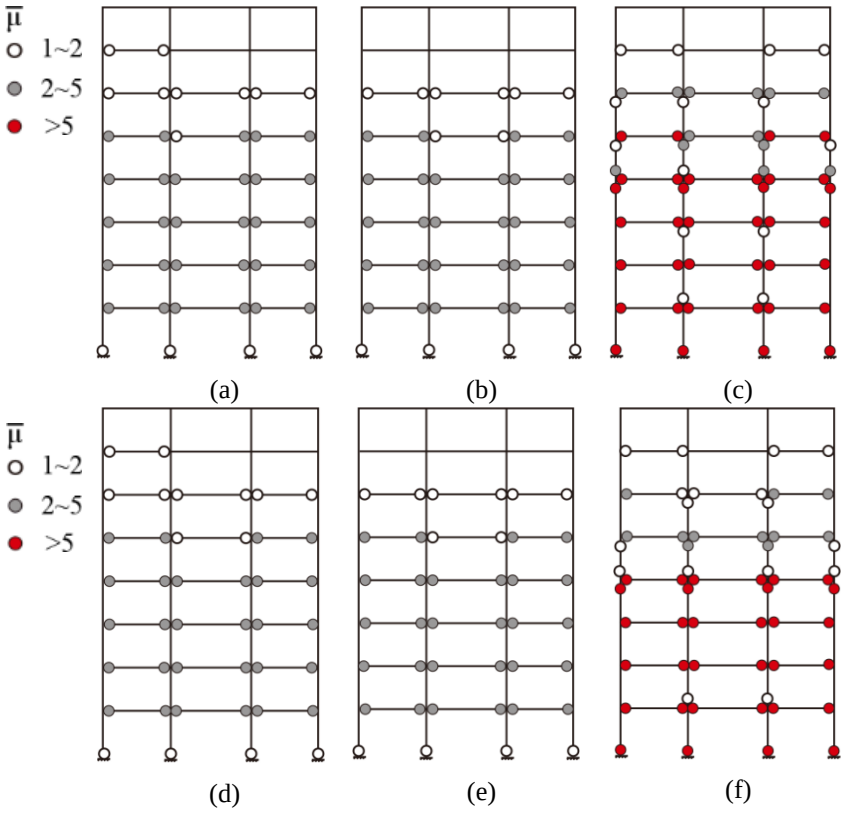

Fig. 4 Comparisons of structural local damage (PGA=0.5g): (a) far-field EQ with Model-1; (b) near-field EQ with Model-1; (c) near-field-P EQ with Model-1; (d) far-field EQ with Model-2; (e) near-field EQ with Model-2; and (f) near-field-P EQ with Model-2

3. CONCLUSIONS

In this paper, the influences of strain rate effect on the seismic performance of a RC frame structure designed according to the Chinese seismic design code are numerically investigated. Based on the empirical formulas of the DIFs, an effective approach for considering strain rate effect is applied in the nonlinear dynamic analysis of RC structures. The rate-independent and rate-dependent models of are established on the OpenSees platform. The seismic performance of the exemplar frame structure under the earthquakes with different types and intensities is studied through the incremental dynamic analysis method. The numerical results indicated that the strain rate effect has a considerable impact on the global responses and local damage of RC

structure under seismic excitations. Moreover, it is suggested that the strain rate effect should be given great attention in the seismic performance assessment of RC structures subjected to high-intensity pulse-like earthquakes. The conclusions drawn in this paper can provide a theoretical reference to further study in this field.

REFERENCES

Adhikary, S.D., Li, B. and Fujikake, K. (2012), "Dynamic behavior of reinforced concrete beams under varying rates of concentrated loading," *Int. J. Impact. Eng.,* **47**(4), 24-38.

Al-Haddad, M.S. (1995), "Curvature ductility of reinforced concrete beams under low and high strain rates," *ACI Mater. J.*, **92**(5), 526-534.

Asprone, D., Frascadore, R., Ludovico, M.D., Prota, A. and Manfredi, G. (2012), "Influence of strain rate on the seismic response of RC structures," *Eng. Struct.,* **35**, 29-36.

Fu, H.C., Erki, M.A. and Seckin, M. (1991), "Review of effects of loading rate on reinforced concrete," *J. Struct. Eng., ASCE,* **117**(12), 3660-3679.

GB50011-2010 (2010), *Code for seismic design of buildings*, Ministry of Construction of China, Beijing (in Chinese).

Ghannoum, W., Saouma, V., Haussmann, G., Polkinghorne, K., Eck, M. and Kang, D.H. (2012), "Experimental investigations of loading rate effects in reinforced concrete columns," *J. Struct. Eng., ASCE,* **138**(8), 1032-1041.

The Euro-International Committee for Concrete (1993), *CEP-FIP model code 1990, Lausanne*, Thomas Telford Ltd.

Li, M. and Li, H.N. (2012), "Effects of strain rate on reinforced concrete structure under seismic loading," *Adv. Struct. Eng.,* **15**(3), 461-476.

Li, R.H., Li, H.N. and Li., C. (2018), "Seismic performance assessment of RC frame structures subjected to far-field and near-field ground motions considering strain rate effect," *Int. J. Struct. Stab. Dy.,* **18**(10), 1850127-1-23.

Liao, W.I, Loh, C.H., Lee, B.H. (2004), "Comparison of dynamic response of isolated and non-isolated continuous girder bridges subjected to near-fault ground motions," *Eng. Struct.,* **26**(14), 2173-2183.

Pankaj, P. and Lin, E. (2005), "Material modelling in the seismic response analysis for the design of RC framed structures," *Eng. Struct.,* **27**(7), 1014-1023.

Qu, Z., Wada, A., Motoyui, S., Sakata, H. and Kishiki, S. (2012), "Pin-supported walls for enhancing the seismic performance of building structures," *Earthq. Eng. Struct. D.*, **41**(14), 2075–2091.

Stewart, J.P., Chiou, S.J., Bray, J.D., Graves, R.W. (2002), " Ground motion evaluation procedures for performance-based design," *Soil. Dyn. Earthq. Eng.,* **22**(9): 765-772.

Wang, C., Xiao, J. and Sun, Z. (2016), "Seismic analysis on recycled aggregate concrete frame considering strain rate effect," *Int. J. Conc. Struct. Mater.,* **10**(3), 307-323.

Wang, D.B., Li, H.N. and Li, G. (2013), "Experimental study on dynamic mechanical properties of reinforced concrete column," *J. Reinf. Plast. Comp.* **32**(23), 1793-1806.

Zhang, H. and Li, H.N. (2011), "Dynamic analysis of reinforced concrete structure with strain rate effect," *Mater. Res. Innov.* **15**(s1), s213-s216.